JVI Journals.ASM.org

Human Parvovirus B19 DNA Replication Induces a DNA Damage Response That Is Dispensable for Cell Cycle Arrest at Phase G_2/M

Sai Lou,[a,b] Yong Luo,[b] Fang Cheng,[b] Qinfeng Huang,[b] Weiran Shen,[b] Steve Kleiboeker,[c] John F. Tisdale,[d] Zhengwen Liu,[a] and Jianming Qiu[b]

Department of Infectious Diseases, First Affiliated Hospital, School of Medicine, Xi'an Jiaotong University, Xi'an, China[a]; Department of Microbiology, Molecular Genetics and Immunology, University of Kansas Medical Center, Kansas City, Kansas, USA[b]; ViraCor-IBT Laboratories, Lee's Summit, Missouri, USA[c]; and Molecular and Clinical Hematology Branch, National Institute of Diabetes and Digestive and Kidney Diseases, National Heart, Lung, and Blood Institute, National Institutes of Health, Bethesda, Maryland, USA[d]

Human parvovirus B19 (B19V) infection is highly restricted to human erythroid progenitor cells, in which it induces a DNA damage response (DDR). The DDR signaling is mainly mediated by the ATR (ataxia telangiectasia-mutated and Rad3-related) pathway, which promotes replication of the viral genome; however, the exact mechanisms employed by B19V to take advantage of the DDR for virus replication remain unclear. In this study, we focused on the initiators of the DDR and the role of the DDR in cell cycle arrest during B19V infection. We examined the role of individual viral proteins, which were delivered by lentiviruses, in triggering a DDR in *ex vivo*-expanded primary human erythroid progenitor cells and the role of DNA replication of the B19V double-stranded DNA (dsDNA) genome in a human megakaryoblastoid cell line, UT7/Epo-S1 (S1). All the cells were cultured under hypoxic conditions. The results showed that none of the viral proteins induced phosphorylation of H2AX or replication protein A32 (RPA32), both hallmarks of a DDR. However, replication of the B19V dsDNA genome was capable of inducing the DDR. Moreover, the DDR *per se* did not arrest the cell cycle at the G_2/M phase in cells with replicating B19V dsDNA genomes. Instead, the B19V nonstructural 1 (NS1) protein was the key factor in disrupting the cell cycle via a putative transactivation domain operating through a p53-independent pathway. Taken together, the results suggest that the replication of the B19V genome is largely responsible for triggering a DDR, which does not perturb cell cycle progression at G_2/M significantly, during B19V infection.

Human parvovirus B19 (B19V) is a small nonenveloped virus with a single-stranded DNA (ssDNA) genome of 5.6 kb (18) and belongs to the genus *Erythrovirus* in the family *Parvoviridae* (68). B19V infection in healthy adults is self-limiting, but in immunocompromised individuals, those with inherited hemolytic anemia, and pregnant women, B19V infection can cause aplastic crisis and hydrops fetalis, which can be fatal (74). B19V infection is restricted to human erythroid progenitor cells (EPCs) (2, 44, 51, 63). During B19V infection, nine major mRNA transcripts are generated by alternative processing of a single precursor mRNA (50) and encode one large nonstructural 1 (NS1) protein, two small nonstructural proteins (11-kDa and 7.5-kDa proteins), and two capsid proteins (VP1 and VP2) (37, 64, 78). The NS1 protein is essential for B19V DNA replication (78) and is a transactivator for viral gene expression (22, 25, 55), as well as for the expression of several cellular genes (24, 41, 48). NS1 is also thought to induce cell cycle arrest (45, 70) and apoptosis (42) of infected EPCs. The 11-kDa protein plays a role in the viral DNA replication (78) and apoptosis induced during infection (13); however, the function of the 7.5-kDa protein remains unknown. Apart from serving as a minor structural protein (30), VP1 also contains a unique region that is essential for the intracellular trafficking of the virus into the nucleus (75). VP2 is the major structural protein involved in virion formation (30, 31).

Ex vivo-expanded EPCs are highly permissive for B19V infection (62, 72) and support an efficient productive B19V infection when EPCs are cultured under hypoxic conditions (10, 53). A few erythropoietin-dependent cell lines, e.g., the megakaryoblastoid cell line UT7/Epo-S1 (S1) (47), support B19V infection with limited efficiency; however, replication of the B19V genome is increased approximately 100-fold when S1 cells are cultured under hypoxic conditions (10). After B19V infection, host cells show remarkable responses to viral infection. B19V induces a DNA damage response (DDR) (39), cell cycle arrest (45–47, 70), and cell death (13, 42, 46, 73), among which the B19V-induced DDR is hijacked by the virus to promote viral DNA replication (39). Three phosphatidylinositol 3-kinase-like kinases (PI3Ks), ataxia telangiectasia-mutated (ATM), ataxia telangiectasia-mutated and Rad3-related (ATR), and the DNA-dependent protein kinase catalytic subunit (DNA-PKcs) are activated; however, the ATR is the major determinant for the DDR induced during B19V infection, and both the ATR and DNA-PKcs are essential for promoting viral genome replication (39). Which viral components are responsible for triggering the DDR and whether the induced DDR is detrimental to host cells during B19V infection are currently unknown.

DDR involves biochemical pathways that arrest cell cycle progression in response to DNA damage or replication stress. Activation of ATR or ATM phosphorylates downstream factors to induce cell cycle arrest and facilitate DNA repair (7, 35). As B19V infection activates the ATR and ATM signaling pathways, they presumably contribute to G_2/M arrest during B19V infection.

Received 23 April 2012 Accepted 17 July 2012
Published ahead of print 25 July 2012
Address correspondence to Jianming Qiu, jqiu@kumc.edu, or Zhengwen Liu, liuzhengwen2011@gmail.com.

doi:10.1128/JVI.01007-12

However, pharmacological inhibitors of DDR do not rescue G_2/M arrest in infected cells, although viral DNA replication is significantly decreased (39). In contrast, the B19V NS1 plays a key role in inducing G_2/M arrest during B19V infection in EPCs through the interaction between its nuclear localization signal (NLS) domain and the cellular transcription factors E2F4/E2F5 (70). It is arguable that DDR signaling and the interaction between NS1 and E2F4/E2F5 are redundant for arresting B19V-infected cells at the G_2/M phase; nevertheless, the role of the DDR in cell cycle perturbation during B19V infection needs to be confirmed.

We recently demonstrated that hypoxic conditions promote efficient B19V infection in both EPCs and S1 cells (10). B19V infection of EPCs under hypoxic conditions *in vitro* mimics B19V infection of EPCs in the human bone marrow and fetal liver, where such hypoxic conditions exist (16, 52, 58, 67). To understand the cause of the DDR and to differentiate the role of the DDR from that of NS1 in inducing G_2/M arrest, in this study we cultured both S1 cells and EPCs under hypoxic conditions; EPCs were transduced with lentiviruses expressing individual viral proteins, and S1 cells were transfected with the double-stranded DNA (dsDNA) form of the B19V ssDNA genome.

MATERIALS AND METHODS

Cells and virus infection. Primary human $CD34^+$ cells were isolated from granulocyte colony-stimulating factor (G-CSF)-mobilized peripheral blood stem cells from healthy donors according to a protocol (02-H-0160) approved by the National Heart, Lung, and Blood Institute institutional review board. EPCs were expanded *ex vivo* from the primary human $CD34^+$ cells in Wong medium as previously described (9, 72). Briefly, cells frozen on day 4 of culture were thawed and cultured under normoxic conditions until day 7. The cells were then transferred to hypoxic conditions (1% O_2 and 5% CO_2) for 48 h before infection or transduction (10). The S1 cells were cultured as described previously (26) and kept under hypoxic conditions for 48 h before electroporation, B19V infection, or lentiviral transduction.

The B19V plasma sample (no. P158, $\sim 1 \times 10^{11}$ genome copies [gc]/ml) was supplied by the ViraCor-IBT Laboratories (Lee's Summit, MO). B19V infection was carried out at a multiplicity of infection (MOI) of 1,000 gc/cell by following the methods previously described (10).

Transfection. The electroporation of S1 cells was performed as previously described (26). The B19V dsDNA genome (M20) and its derivative mutants were recovered from SalI-digested pIB19-M20 and its derivative mutants.

Plasmid construction. (i) Lentiviral vectors. The DNA coding sequences for the B19V NS1, 11-kDa, 7.5-kDa, VP1, and VP2 proteins were optimized at GenScript USA Inc. (Piscataway, NJ) to enhance protein expression efficiency (79). The pLenti-CMV-IRES-GFP-WPRE vector (36) was used for inserting C-terminally Flag-tagged optimized (opt) NS1-, 11-kDa protein-, 7.5-kDa protein-, VP1-, and VP2-coding sequences at BamHI and BsrGI sites, resulting in the following constructs: pLenti-optNS1, pLenti-opt11-kDa, pLenti-opt7.5-kDa, pLenti-optVP1, and pLenti-optVP2.

The B19V P6 promoter-based NS1-expressing lentiviral vector, pLenti-½ITR-P6-NS1, was constructed as follows: a DNA fragment from nucleotides 187 to 2628 of the B19V genome, which spans the left half of the inverted terminal repeat (ITR), namely, ½ITR, the P6 promoter, and the NS1-encoding sequence, with a Flag epitope at the C terminus, was inserted into ClaI/SalI-digested pLenti-CMV-GFP-WPRE, which was made by removing the puromycin gene expression cassette from pLenti-GFP-Puro (Addgene Inc., Cambridge, MA). The amino acid sequence of B19V NS1 (GenBank accession no. AAQ91878.1) was aligned with that of adeno-associated virus 2 (AAV2) Rep78 (GenBank accession no. AAC03775.1), which locates the conserved endonuclease domain (69) and helicase Walker A box site (43, 69) in the B19V NS1 (see Fig. 2C). Putative transactivation domains (TADs) at the C terminus of the B19V NS1 were predicted by the 9aaTAD program (54) (see Fig. 3A). Then, mutations of the putative endonuclease and helicase-A domains and the predicted TAD2 and TAD3 were introduced into the NS1-encoding region of pLenti-½ITR-P6-NS1, constructing pLenti-½ITR-P6-NS1(endo-), pLenti-½ITR-P6-NS1(heli-), pLenti-½ITR-P6-NS1(mTAD2), and pLenti-½ITR-P6-NS1(mTAD3), respectively. pLenti-½ITR-P6-RFP was made by replacing the NS1-encoding sequence with a red fluorescent protein (RFP) open reading frame (ORF) (13).

(ii) Mutants of pIB19-M20. The B19V infectious clone pIB19-M20 (80), NS1 knockout mutant [pIB19-M20($NS1^-$)], and VP2 knockout mutant [pIB19-M20(VP^-)] (78) were gifts from Kevin Brown and Ning Zhi at the NIH. The M20 DNA is a dsDNA form of the B19V ssDNA genome, which presumably is an intermediate replicative form (RF) of the B19V genome during virus replication (27). Mutations of the putative endonuclease and helicase-A domains and the predicted TAD1, TAD2, and TAD3 of NS1 (see Fig. 2C and 3A) were introduced into pIB19-M20, creating pIB19-M20($endo^-$), pIB19-M20($heli^-$), and pIB19-M20(mTAD1, mTAD2, and mTAD3).

(iii) pLKO-shRNA vectors. The validated coding sequence for p53 short hairpin RNA (shRNA) was obtained from Sigma (St. Louis, MO) as follows: 5′-CCG GTC GGC GCA CAG AGG AAG AGA ATC TCG AGA TTC TCT TCC TCT GTG CGC CGT TTT TC-3′ (clone identifier, NM_000546.x-1095s1c1). pLKO-shRNA-p53 was made by inserting a DNA fragment of this sequence into the AgeI/EcoRI-digested pLKO-GFP-scramble-shRNA vector (Addgene Inc.) as described previously (9).

All the nucleotide numbers of the B19V genome refer to GenBank accession no. AY386330.

First antibodies used. Rat anti-B19V NS1 (anti-NS1) and anti-11-kDa protein polyclonal antibodies were previously reported (13, 39). Mouse anti-7.5-kDa protein polyclonal antibody was made by immunizing mice with purified glutathione *S*-transferase-fused 7.5-kDa protein by following the method previously described (36). The following antibodies were obtained commercially: anti-VP1/VP2 antibody (MAB8292, Millipore, Billerica, MA), anti-phosphorylated H2AX (γ-H2AX) antibodies (05-636, Millipore; 2212-1, Epitomics, Burlingame, CA), anti-phosphorylated replication protein A32 (p-RPA32) (3237-1, Epitomics), anti-p53 antibody (GTX102965, GeneTex, Irvine, CA), anti-Flag antibody (200472, Agilent Technologies, Santa Clara, CA), and anti-β-actin antibody (A5441, Sigma-Aldrich, St. Louis, MO).

Lentivirus production and transduction. Lentiviruses were generated as previously described (36). EPCs were transduced at an MOI of approximately 10/cell as previously described (9), whereas S1 cells were transduced at an MOI of 1/cell. S1 cells were preincubated with p53-shRNA lentivirus by slow rotation at 4°C for 1.5 h before culture at 37°C.

Immunofluorescence analysis. Immunofluorescence (IF) staining was performed as previously described (39). Texas Red-conjugated donkey anti-rat antibody (catalog no. 712-076-153) was used for NS1 or 11-kDa protein detection, and fluorescein isothiocyanate (FITC)-conjugated donkey anti-mouse antibody (catalog no. 715-095-151) was used for γ-H2AX (anti-γ-H2AX, Millipore) or Alexa Fluor 488-conjugated donkey anti-rabbit antibody (catalog no. 711-546-152) was used for p-RPA32. Rhodamine red-X-conjugated donkey anti-mouse antibody (catalog no. 715-295-150) was used for 7.5-kDa protein or VP1/VP2 detection, and Alexa Fluor 488-conjugated donkey anti-rabbit antibody (catalog no. 711-546-152) was used for γ-H2AX (anti-γ-H2AX, Epitomics) or p-RPA32. All the secondary antibodies were purchased from Jackson ImmunoResearch Laboratories (West Grove, PA).

Images were taken under a confocal microscope (Eclipse C1 Plus, Nikon) with Nikon EZ-C1 software.

Flow cytometry analysis. Cells were stained and analyzed by flow cytometry as previously described (11, 36). For cell cycle analysis of the B19V-infected S1 cells and EPCs and of S1 cells transfected with M20 and its mutants, cells were fixed, permeabilized, and costained 48 h postinfec-

tion (p.i.) or posttransfection (p.tx.) in succession with the rat anti-NS1 antibody, a Cy5-conjugated goat anti-rat antibody (catalog no. 112-176-143) for detection of NS1, and 4′,6-diamidino-2-phenylindole (DAPI). For cell cycle analysis of the lentivirus-transduced S1 cells and EPCs, cells were stained 48 h posttransduction (p.td.) with the mouse anti-Flag antibody, followed by a Dylight 649-conjugated goat anti-mouse antibody (catalog no. 115-496-003) and DAPI.

To determine the level of a DDR, S1 cells were fixed, permeabilized, and costained 48 h p.i./p.tx. with the mouse anti-γ-H2AX (Millipore) and rat anti-NS1 antibodies, followed by FITC-conjugated donkey anti-mouse (catalog no. 715-095-151) and Alexa Fluor 647-conjugated donkey anti-rat (catalog no. 712-606-153) secondary antibodies for the detection of γ-H2AX and NS1, respectively. All of the secondary antibodies were purchased from Jackson ImmunoResearch Laboratories.

All of the samples were analyzed on a three-laser flow cytometer (LSR II, BD Biosciences) at the Flow Cytometry Core of the University of Kansas Medical Center. All flow cytometry data were analyzed using FACSDiva software (BD Biosciences).

Southern blot analysis. Low-molecular-weight (Hirt) DNA was extracted from treated cells, followed by DpnI digestion and Southern blotting as previously described (26) with M20 DNA as a probe template. Images were developed and analyzed with a Typhoon 9700 phosphorimager (GE Healthcare).

SDS-PAGE and Western blot analysis. Sodium dodecyl sulfate-polyacrylamide gel electrophoresis (SDS-PAGE) was performed as previously described (13). For Western blotting, cell lysates were prepared and analyzed as previously described (36).

RESULTS

Individual B19V viral protein does not induce a DDR in EPCs. We previously reported that B19V infection induces a DDR in infected EPCs cultured under normoxic conditions (39). Since hypoxic conditions promote the infection of EPCs by B19V (10), we cultured EPCs under hypoxic conditions and infected them with B19V. B19V infection of EPCs cultured under hypoxic conditions also induced a DDR, as evidenced by the phosphorylation of both H2AX and RPA32 (which are hallmarks of the DDR [5, 40, 65]), at levels approximately three times higher than those in infected cells cultured under normoxic conditions (Fig. 1A). Notably, p53 was phosphorylated in B19V-infected EPCs under normoxic conditions and phosphorylated further under hypoxic conditions.

Since B19V expresses the nonstructural proteins (NS1, 7.5-kDa protein, and 11-kDa protein) in addition to the structural proteins (VP1 and VP2) during infection (37, 64, 78), we examined whether the expression of the individual viral proteins induced a DDR in EPCs. We expressed the nonstructural proteins and structural proteins in EPCs via lentiviral transduction. As a positive control for the DDR, EPCs were treated with hydroxyurea (HU). At 48 h p.td., EPCs were analyzed for the expression of phosphorylated H2AX and RPA32 by IF staining. B19V-infected EPCs showed pan-distribution of γ-H2AX (Fig. 1B) and colocalized foci of NS1 with p-RPA32 (Fig. 1C) in the nuclei, which was consistent with that in infected EPCs cultured under normoxic conditions (39). However, we observed that NS1 was expressed in the cytoplasm to a greater extent than in the nucleus, likely due to the high infectivity of B19V in EPCs cultured under hypoxic conditions (10). In contrast to the formation of nuclear foci during B19V infection, NS1-transduced EPCs showed neither phosphorylation of H2AX nor colocalization of NS1 and p-RPA32 (Fig. 1B and C). A proportion of the NS1 in transduced EPCs appeared to be in the cytoplasm, mimicking the NS1 expression pattern observed during viral infection. The difference in γ-H2AX and p-RPA32 expression between B19V-infected and NS1-transduced EPCs suggests that B19V NS1 alone is not sufficient to induce the DDR observed during B19V infection. Similarly, when the 7.5-kDa, 11-kDa, VP1, and VP2 proteins were expressed in EPCs by their respective lentiviruses, neither H2AX nor RPA32 was phosphorylated in transduced EPCs (Fig. 1B and C), whereas HU treatment of control cells induced the phosphorylation of both H2AX and RPA32.

Taken together, these results confirm that B19V viral proteins, including NS1, the 7.5-kDa protein, the 11-kDa protein, VP1, and VP2, alone do not induce the DDR in EPCs that is observed during B19V infection.

Replication of the B19V dsDNA genome induces a DDR in S1 cells. Hypoxic conditions support the efficient replication of the B19V dsDNA genome (M20 DNA) in S1 cells at a level approximately 100 times greater than that observed under normoxic conditions (10). Since B19V replication in EPCs requires a DDR (39), we hypothesized that the replication of B19V M20 DNA in S1 cells induces a DDR as well. To this end, S1 cells were transfected with M20 and a mutant [M20(VP$^-$)] in which the VP2 ORF was knocked out and neither VP1 nor VP2 was expressed (data not shown). Cells were infected with B19V as a control. We found that both wild-type M20-transfected and B19V-infected S1 cells generated DpnI digestion-resistant bands of ssDNA, monomer RF (mRF) DNA, and double RF (dRF) DNA on a Southern blot (Fig. 2A). This indicated that B19V M20 DNA replicated in the transfected cells. The negative control, M20(NS1$^-$)-transfected cells, did not generate any DpnI digestion-resistant DNA bands, confirming that NS1 is essential for B19V DNA replication. Transfection of mutant M20(VP$^-$) yielded clear mRF and dRF DNA bands but not ssDNA bands (Fig. 2A, lane 4). Production of ssDNA was significantly inhibited in the absence of capsid proteins during B19V DNA replication. When the putative endonuclease domain or helicase-A site was mutated, the M20(endo$^-$) and M20(heli$^-$) mutants did not replicate in transfected cells, as evidenced by the lack of DpnI digestion-resistant DNA bands (Fig. 2B, lanes 3 and 4).

The transfection of M20 induced phosphorylation of both H2AX and RPA32 and induced the formation of NS1 and p-RPA32 foci in the nuclei of transfected cells, similar to that observed in B19V-infected S1 cells (Fig. 2D and E). Moreover, H2AX and RPA32 were phosphorylated and colocalized with NS1 in the nuclei of M20(VP$^-$)-transfected S1 cells. Notably, M20(endo$^-$)- and M20(heli$^-$)-transfected NS1-positive (NS1$^+$) cells did not express γ-H2AX (Fig. 2D) or p-RPA32 (Fig. 2E). Next, we carefully quantified the DDR induced in S1 cells infected with B19V or transfected with M20 and its mutants by flow cytometry. Replicative B19V M20 DNAs [M20 and M20(VP$^-$)] and B19V infection induced significant expression of γ-H2AX in NS1-expressing cells (Fig. 2F and G), which was significantly higher than those induced by nonreplicative M20 DNAs [M20(endo$^-$) and M20(heli$^-$)].

Taken together, these results show that replication of B19V M20 DNA *per se*, without ssDNA production, is sufficient to induce a DDR at a level similar to that induced during B19V infection.

B19V DNA replication-induced DDR does not induce G_2/M arrest after transfection. B19V infection of EPCs triggers a DDR cascade with the activation of all three PI 3-kinases (ATM, ATR, and DNA-PKcs) (39). It also arrests infected cells at the G_2/M

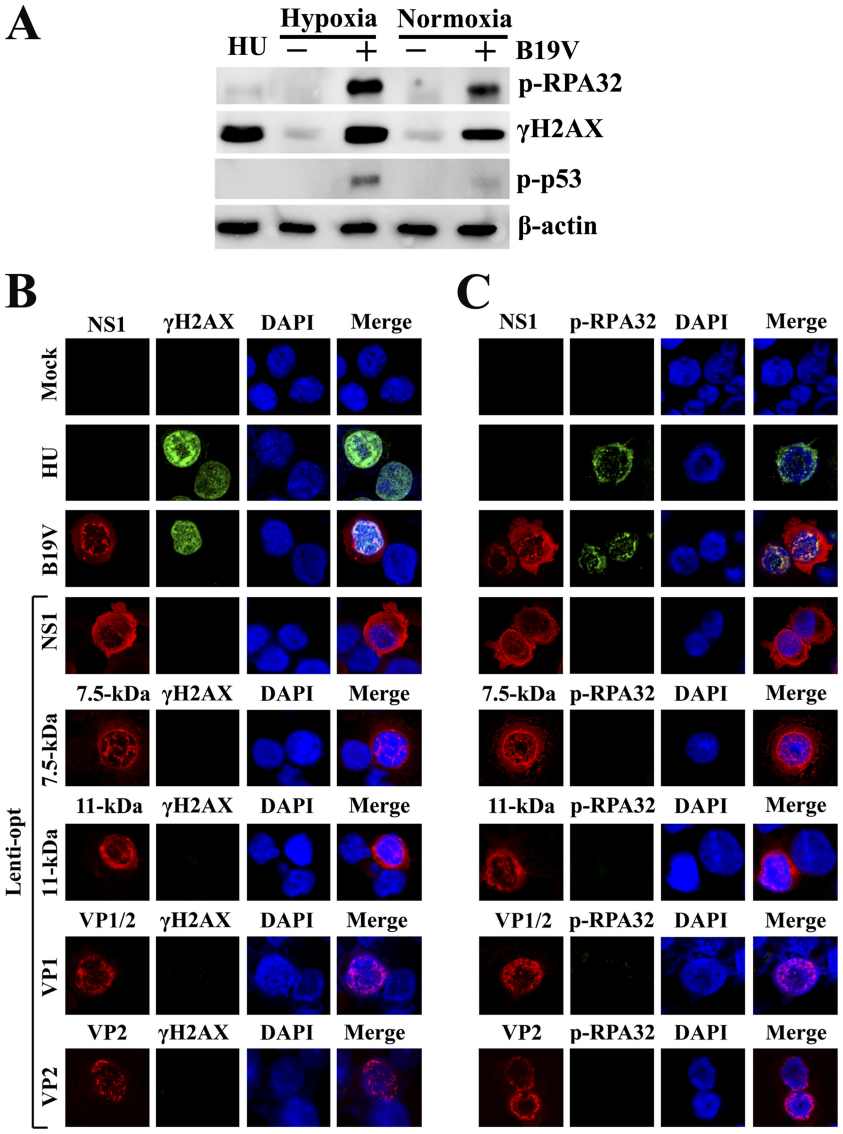

FIG 1 B19V viral proteins do not induce a DDR in EPCs cultured under hypoxic conditions. (A) B19V infection induces a stronger DDR in EPCs cultured under hypoxic conditions than in EPCs cultured under normoxic conditions. EPCs cultured at either normoxic or hypoxic conditions were mock infected (−) or infected with B19V (+) at the same MOI. At 48 h p.i., cells were harvested and analyzed by Western blotting using the indicated antibodies. (B and C) B19V viral proteins do not elicit a DDR individually in EPCs cultured under hypoxic conditions. EPCs cultured under hypoxic conditions were mock infected, infected with B19V, or transduced with the indicated lentiviruses. (B) At 48 h p.i. or p.t.d., cells were fixed and costained with an antiviral protein antibody (red), an anti-γ-H2AX antibody (green), and DAPI (blue). (C) At 48 h p.i. or p.t.d., cells were fixed and costained with an antiviral protein antibody (red), an anti-p-RPA32 antibody (green), and DAPI (blue). Confocal images were taken at a magnification of ×100. Hydroxyurea (HU)-treated EPCs served as a positive control for DDR detection.

phase (70). ATM- and ATR-mediated signaling is thought to be the major pathway leading to cell cycle arrest at the G_2/M checkpoint (35, 61). However, in EPCs the expression of B19V NS1 alone can induce G_2/M arrest (70). Hence, we examined the role of the B19V DNA replication-induced DDR in G_2/M arrest.

We first tried to identify an M20 mutant that replicates but does not induce significant G_2/M arrest in transfected cells. The DNA binding (endonuclease) and helicase domains of NS1 were critical for B19V DNA replication (Fig. 2B), and mutations in the NLS site abolished DNA replication (data not shown). We focused on the C terminus of NS1, particularly the predicted TADs, since the TAD of minute virus of mice (MVM) NS1 is dispensable for MVM DNA replication (33). Three TADs were predicted by analyzing the C terminus of NS1 using a TAD prediction program (54) (Fig. 3A). We mutated each of the predicted TADs in M20 and assessed their replication capability. Only the M20(mTAD2), which harbors mutations in TAD2, replicated in transfected S1 cells at a level comparable with that in the wild type (Fig. 3B, lane 3). Furthermore, we examined the ability of the M20-based TAD mutants to trigger a DDR in transfected cells. The results showed that in only the M20(mTAD2)-transfected ($NS1^+$) cells were both H2AX and RPA32 clearly phosphorylated but not in cells transfected with M20(mTAD1) and M20(mTAD3) (Fig. 3C), supporting the notion that B19V DNA replication is critical for inducing a DDR.

We next tested the ability of wild-type M20 and its mutants to arrest the cell cycle at G_2/M by transfecting them into S1 cells.

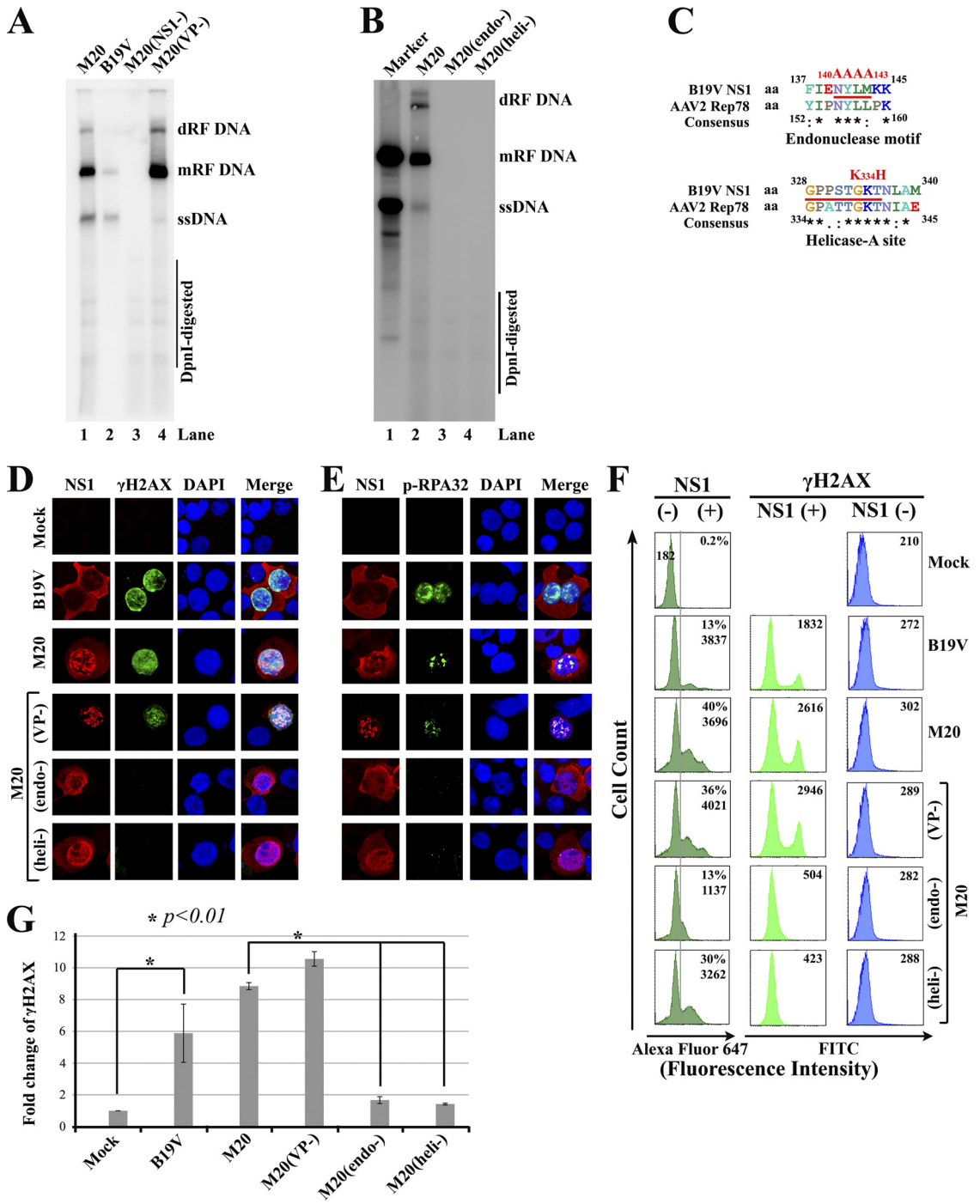

FIG 2 Replication of B19V dsDNA genome induces a DDR in S1 cells. S1 cells, which were precultured under hypoxic conditions for 48 h, were infected with B19V or electroporated with B19V dsDNA genome (M20) or its mutants, as indicated. At 48 h p.i. or p.tx., cells were harvested and analyzed as follows. (A and B) Southern blot analysis. Hirt DNA was extracted from infected or transfected S1 cells and digested with DpnI followed by Southern blotting. In panel B, M20 DNA (10 ng) was used as the size marker. The smaller band detected coincidentally at the site of the ssDNA is likely degraded M20 DNA. mRF, monomer replicative form; dRF, double replicative form. (C) Diagram of the mutations in the endonuclease motif and helicase-A site of the NS1 protein. Amino acid sequences of B19V NS1 (GenBank accession no. AAQ91878.1) and AAV2 Rep78 (AAC03775.1) were aligned using ClustalW2 (32). Asterisks show the consensus sequences in the endonuclease and helicase-A domains, and mutations are shown in red. (D and E) IF staining of the DDR markers. Cells were costained with anti-NS1 (red), anti-γ-H2AX (green) (D) or anti-p-RPA32 (green) (E) antibodies, and DAPI (blue). Confocal images were taken at a magnification of ×100. (F) Flow cytometry analysis. Cells were costained with anti-NS1 antibodies, anti-γ-H2AX antibodies, and their respective secondary antibodies and analyzed by flow cytometry. The *x* axes of all the plots are in logarithmic scale, while the *y* axes are in arithmetic scale. For NS1 staining (left-hand histograms), a reference line was drawn based on the secondary antibody-only control (mock) for a cutoff between the NS1-negative ($NS1^-$) and -positive ($NS1^+$) populations. Both the NS1-positive rate (%) and the mean fluorescence intensity (MFI) of NS1 expression in the $NS1^+$ population are presented in each plot. For γ-H2AX staining, levels of γ-H2AX are shown as the MFI both in the $NS1^+$ and $NS1^-$ cell populations of each group in the middle and right-hand histograms, respectively. The MFI in the mock groups was read from the whole population. (G) Statistical analysis. The fold change of γ-H2AX represents the ratio of the MFI of γ-H2AX for the $NS1^+$ to that for the $NS1^-$ population and is represented as the mean plus or minus the standard deviation from at least three independent experiments. *P* values were determined using Student's *t* test.

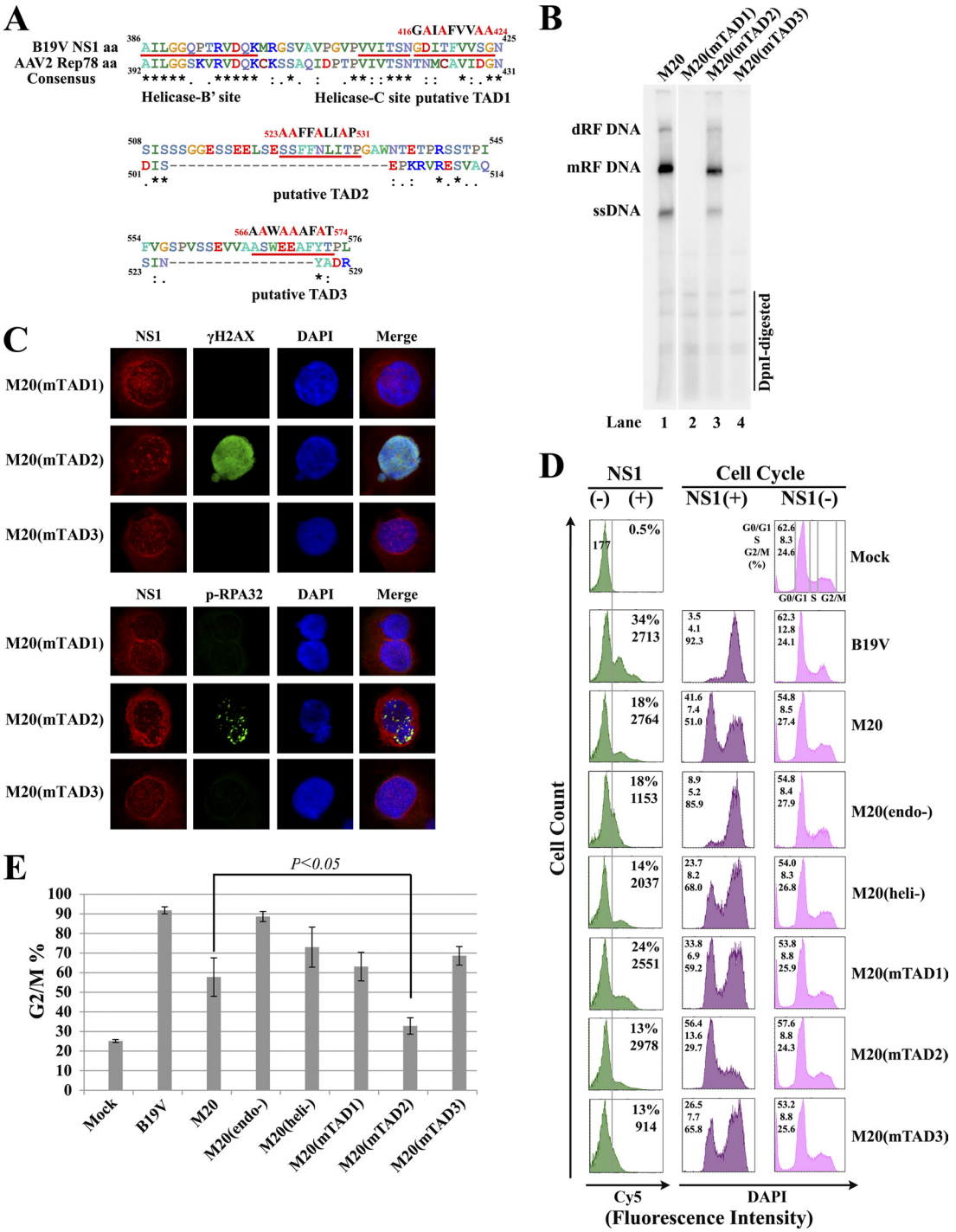

FIG 3 B19V DNA replication-induced DDR is dispensable for G_2/M arrest induced after transfection. (A) Diagram of predicted transactivation domains (TADs) within the C terminus of B19V NS1. The TADs within B19V NS1 were predicted by analyzing the NS1 amino acid sequence using the 9aaTAD program (54). Three predicted TADs are shown with the mutated amino acids indicated in red above the TADs. (B) Southern blot analysis of transfected DNA replication. S1 cells cultured under hypoxic conditions were transfected with M20, M20(mTAD1), M20(mTAD2), or M20(mTAD3). At 48 h p.tx., cells were collected for Hirt DNA preparation followed by Southern blotting. (C) IF staining of the DDR markers. At 48 h p.tx., the transfected cells were costained with anti-NS1 (red), anti-γ-H2AX, or anti-p-RPA32 (green) antibodies and DAPI (blue). Confocal images were taken at a magnification of ×100. (D) Flow cytometry analysis of the cell cycle. M20 and its indicated mutants were electroporated into S1 cells. B19V-infected S1 cells served as a positive control for NS1 detection and cell cycle analysis. At 48 h p.i. or p.tx., cells were costained with an anti-NS1 antibody and a Cy5-conjugated secondary antibody for NS1 detection and DAPI for cell cycle analysis by flow cytometry. The *y* axes for all the plots are in arithmetic scale. The *x* axes for the NS1-staining plots are in logarithmic scale, while those for the remaining DAPI-staining plots are in arithmetic scale. The methods for gating of the $NS1^-$ and $NS1^+$ cell populations are the same as those described in Fig. 2F. The cell cycle was analyzed in both $NS1^+$ and $NS1^-$ populations in each group, as indicated in the middle and right-hand histograms, respectively. The percentage (%) of the cells in each phase of the cell cycle is shown. (E) Statistical analysis. Data for the percentage of cells at the G_2/M phase (G_2/M%) were obtained from at least three independent experiments and are presented as the mean plus or minus the standard deviation. The *P* value was determined using Student's *t* test.

Notably, the M20 mutants that did not replicate induced clear G_2/M arrest at levels similar to or higher than those observed in the wild type, with the percentage of cells in G_2/M phase ranging from 63.1% to 88.6% in $NS1^+$ cells (Fig. 3D and E). More importantly, the replicative TAD mutant, M20(mTAD2), significantly decreased the number of cells at the G_2/M phase compared with that of the wild-type M20 control (32.8% vs. 57.7%, respectively) (Fig. 3E).

Collectively, these results show that replication of the B19V dsDNA genome is not required to induce G_2/M arrest in transfected S1 cells. Since replication of the B19V dsDNA genome is essential for inducing a DDR, we conclude that the DDR is dispensable for G_2/M arrest of the cells in which B19V DNA replicates. The results also suggest that B19V NS1 alone is sufficient to arrest the cell cycle at G_2/M during infection.

Expression of NS1 alone is sufficient to induce G_2/M arrest in S1 cells and EPCs. To examine the sole role of NS1 in inducing G_2/M arrest, we expressed only wild-type NS1 and the NS1 mutants, which originated from the M20 mutants, by lentiviral transduction in S1 cells and EPCs. Transduction of Lenti-½ITR-P6-NS1, in which expression of wild-type NS1 is driven by the native B19V P6 promoter (55), recapitulated G_2/M arrest to the level induced by B19V infection in S1 cells, in which over 90% of $NS1^+$ cells were arrested at the G_2/M phase. This was also observed after the transduction of lentiviruses expressing the NS1 mutants except for NS1(mTAD2) (Fig. 4A). The expression of NS1(mTAD2) increased the number of $NS1^+$ cells at G_2/M only to 36.6%, a level similar to that induced by the expression of the RFP control (42.4%) (Fig. 4C). In EPCs, in agreement with the results observed in S1 cells, both B19V infection and transduction of lentiviruses expressing wild-type NS1 and the NS1 mutants, NS1(endo$^-$), NS1(heli$^-$), and NS1(mTAD3), induced over 90% of $NS1^+$ cells at the G_2/M phase (Fig. 4B). Notably, the expression of NS1(mTAD2) in EPCs resulted in 42.2% of $NS1^+$ cells to arrest at G_2/M, a level close to that induced by expression of the RFP control (35.0%) (Fig. 4D). We noticed that the expression of RFP in the context of Lenti-½ITR-P6-RFP induced a higher number of cells at G_2/M (approximately 40%) than G_2/M-phased cells (approximately 20%) in the mock group in both S1 cells and EPCs. It has been reported that a consensus Toll-like receptor (TLR) ligand sequence (5′-GTTTTGT-3′) exits in the B19V P6 promoter and inhibits proliferation of EPCs by arresting the cell cycle at the S and G_2/M phases (28). We also observed that a lentiviral vector bearing a B19V sequence of nucleotides 187 to 615 (contains ½ITR and the core P6 promoter) arrested the cell cycle at G_2/M (data not shown).

Taken together, these results confirm that the expression of B19V NS1 alone is sufficient to induce nearly complete G_2/M arrest in the context of the B19V P6 promoter and that the predicted TAD2 of NS1 is critical for G_2/M arrest induced by NS1 in both S1 cells and EPCs.

The p53-mediated pathway is not required for G_2/M arrest induced by B19V infection or transfection of the B19V dsDNA genome. ATM and ATR activation during a DDR phosphorylates p53 at Ser^{15} (3, 60). The cyclin-dependent kinase Cdk1, which controls the G_2/M transition, is inhibited by the product of the p53-targeting gene, p21 (6). Since B19V NS1 transactivates the expression of p21 (45) and p53 is phosphorylated at Ser^{15} during B19V infection of EPCs (70) (Fig. 1A), we decided to examine the role of p53 in B19V-induced G_2/M arrest.

We first attempted to knock out p53 in EPCs using p53-specific shRNAs, which proved to be very difficult (data not shown). Fortunately, nearly perfect p53 knockout was obtained in S1 cells transduced with a p53-shRNA-expressing lentivirus (Fig. 5A). We found that the percentage of p53-deficient $NS1^+$ cells (either infected with B19V or transfected with M20) at the G_2/M phase did not decrease compared with that in scramble (scr)-shRNA-treated cells (Fig. 5B and C), suggesting that the p53-mediated pathway is not used to induce G_2/M arrest during infection or transfection. We also observed that the transfection of M20 caused fewer cells to arrest at G_2/M than B19V infection (56.8% vs. 90.6%) (Fig. 5B); however, knockout of p53 did not ameliorate G_2/M arrest significantly under either condition (Fig. 5C).

DISCUSSION

In this study, we report that the replication of the B19V dsDNA genome, but not the individual viral proteins, induces a DDR. We identified an M20 mutant, M20(mTAD2), containing a mutated transactivation domain within NS1, which replicated well in S1 cells but did not arrest the cell cycle at the G_2/M phase. In agreement with this result, the NS1 harboring the TAD2 mutation did not induce significant G_2/M arrest in either EPCs or S1 cells by lentiviral transduction. Finally, we showed that the p53-mediated pathway is not involved in G_2/M arrest during B19V infection. Thus, our results provide evidence that the DDR induced during B19V infection does not contribute to G_2/M arrest and confirm that NS1 alone is sufficient to induce the G_2/M arrest in the context of the B19V P6 promoter.

A DDR is a response by the cellular surveillance network that senses and repairs damaged DNA and is required to maintain genome integrity (14). During viral infection, a DDR plays a role in the intrinsic antiviral mechanism to eliminate the invasion of the viral genome; however, in some cases, the virus exploits the DDR signaling mechanism to promote its own replication (71). One of the major consequences of a DDR is cell cycle arrest, which ensures that there is time for DNA repair after DNA damage (57). B19V infection of both EPCs and S1 cells typically arrests the cell cycle at G_2/M (39, 47, 70). Preventing replication of the B19V dsDNA genome by mutating the endonuclease domain or helicase-A motif within NS1, which prohibits the DDR, did not reduce the percentage of cells arrested at G_2/M; however, mutating TAD2 could result in a replication-competent M20 mutant but with reduced G_2/M arrest. NS1 alone is sufficient to cause G_2/M arrest, which requires a predicted TAD2. Therefore, B19V utilizes the mechanism of a DDR only to promote viral DNA replication (39), and the NS1-induced G_2/M arrest is dispensable for viral DNA replication. The role of the NS1-induced G_2/M arrest during B19V infection warrants further investigation. The fact that the p53 pathway is not used by B19V NS1 to arrest the cell cycle indicates that the TAD2 of NS1 does not transactivate p53-regulating genes. NS1 expression in EPCs upregulates 44 genes and downregulates 28 genes that are involved in cell cycle regulation (70). Therefore, we hypothesize that TAD2 of NS1 may play an important role in regulating one or several of these genes. The NLS domain of NS1 is thought to be critical for inducing G_2/M arrest, which is mediated by the interaction between NS1 and E2F4/E2F5 (70); however, mutation of the NLS, which prevents NS1 transport into the nucleus (70), may also prevent the function of the TAD. Clearly, our results highlight a novel mechanism underlying

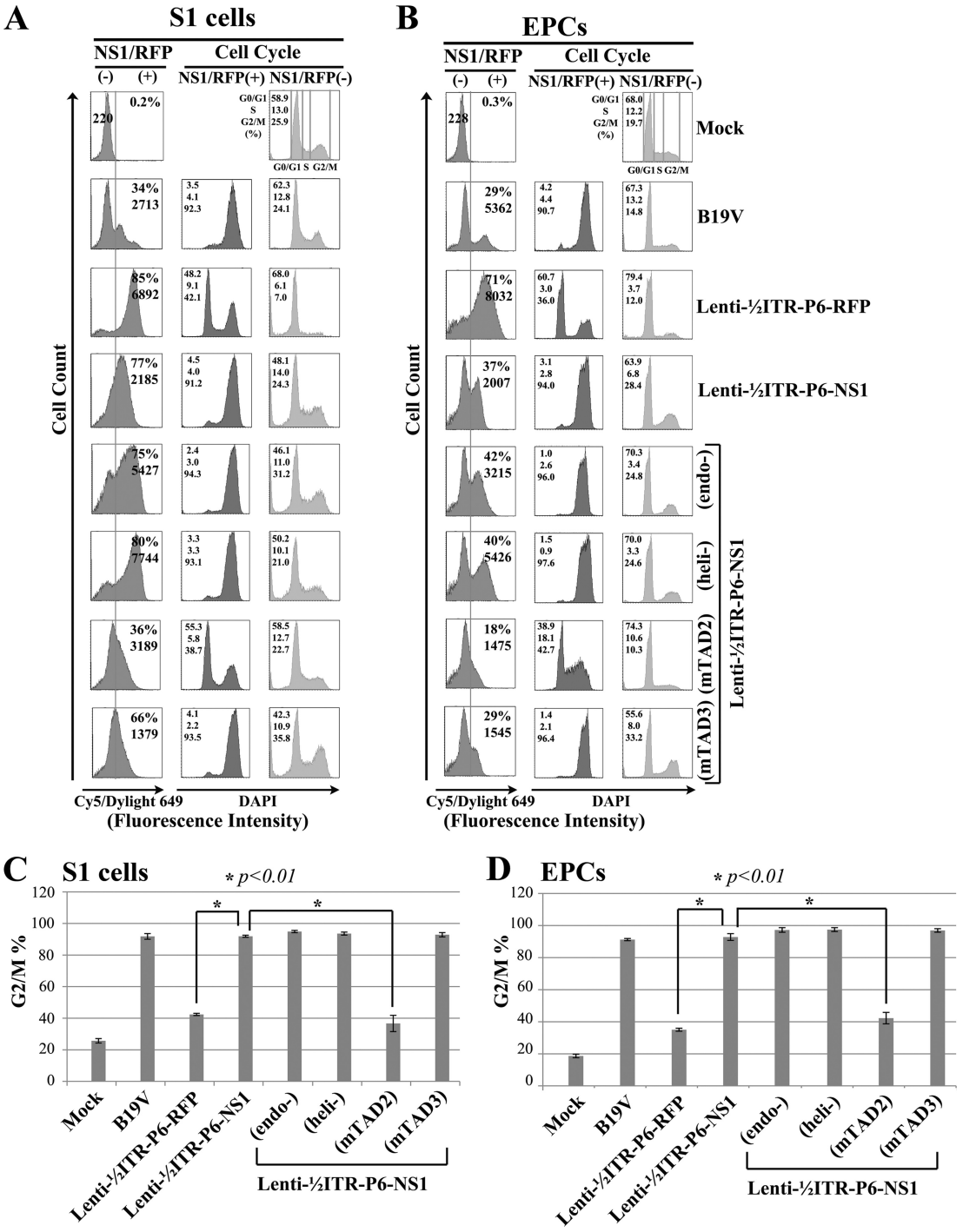

FIG 4 NS1 alone is sufficient to induce G_2/M arrest in S1 cells and EPCs. (A and B) Flow cytometry analyses of S1 cells and EPCs transduced with lentiviruses. S1 cells (A) or EPCs (B) cultured under hypoxic conditions were either infected with B19V or transduced with the indicated lentiviruses. The Lenti-½ITR-P6-RFP serves as a lentiviral control. At 48 h p.i. or p.td., cells were costained with anti-NS1 and Cy5-conjugated secondary antibodies (for B19V-infected cells) or anti-Flag and Dylight 649-conjugated secondary antibodies (for lentivirus-transduced cells), followed by DAPI for cell cycle analysis. NS1 staining and cell cycle analyses were performed as described in Fig. 3D. (C and D) Statistical analysis. Statistical data of the G_2/M% were obtained from at least three independent experiments in S1 cells (C) and EPCs (D), indicated as the mean plus or minus the standard deviation. The *P* values were determined using Student's *t* test.

G_2/M arrest induced by NS1 during B19V infection, which is independent of the DDR and p53 activation.

Viral proteins often play an important role in triggering a DDR during infection (8, 34, 71), particularly in the large T antigen of polyomaviruses (21, 49, 77) and the Vpr of HIV (76). In parvoviruses, the replication of the AAV2 genome during coinfection with adenovirus elicits an ATM-, ATR-, and DNA-PKcs-mediated DDR (17, 59). We reported that DNA replication of the minute

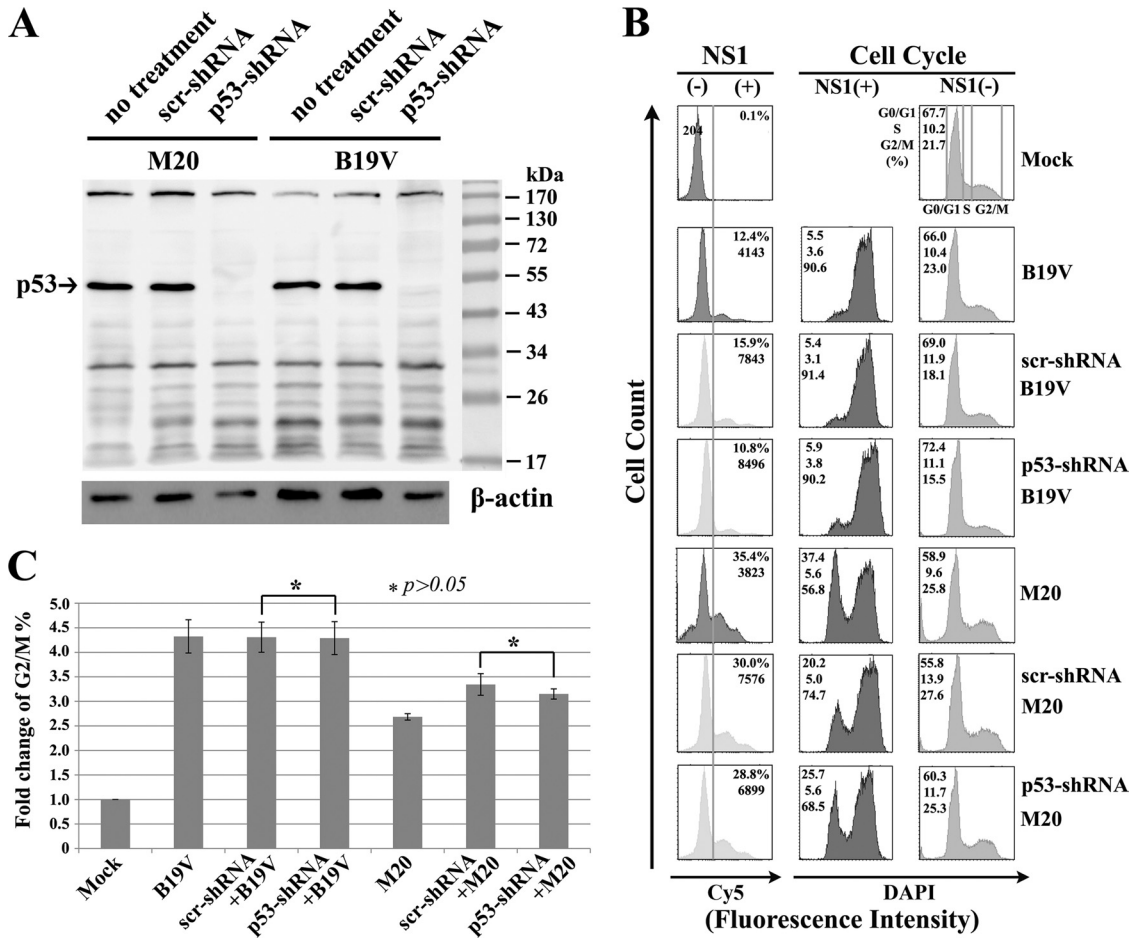

FIG 5 The p53 pathway is not necessary for B19V-induced G_2/M arrest. S1 cells cultured under normoxic conditions were transduced with p53-shRNA- and scramble-shRNA (scr-shRNA)-expressing lentiviruses, which also expressed GFP (9), and then cultured under hypoxic conditions for 48 h. The cells then were mock infected, infected with B19V, or transfected with M20. (A) Western blot analysis of p53 expression. At 48 h p.i. or p.tx., cells were analyzed for the expression of p53 by Western blotting. The blot was probed with an anti-p53 antibody, stripped, and reprobed to examine the β-actin levels. "No treatment" indicates cells not transduced with lentivirus. The arrow indicates the p53 band. (B) Flow cytometry analysis of the cell cycle. At 48 h p.i. or p.tx., cells were costained with the anti-NS1 antibody and Cy5-conjugated secondary antibodies for NS1 detection and DAPI for cell cycle analysis by flow cytometry as described in Fig. 3D. In the shRNA-treated groups, shRNA-expressing cells were selected based on the GFP signal expressed by the lentiviral vector and shown in the left-hand histograms. (C) Statistical analysis of the cell cycle results. The ratio of the percentage of cells at G_2/M (G_2/M%) in the $NS1^+$ population to that in the $NS1^-$ population in each group is named as the fold change of the G_2/M%. Statistical data of the fold change of the G_2/M% were obtained from at least three independent experiments, indicated as the mean plus or minus the standard deviation. The *P* values were determined using Student's *t* test.

virus of canines (MVC) genome is responsible for an MVC-induced DDR rather than the viral proteins (38). The MVM also induces a DDR during infection (1, 56), but the small nonstructural protein NS2 is dispensable (56). The AAV2 Rep78 induces a DDR by introducing nicks in the cellular chromatin (4), but it is only a minor contributor to the DDR induced during AAV2 infection (59). The present study shows that B19V NS1, the small nonstructural proteins (7.5-kDa and 11-kDa proteins), and the capsid proteins failed to induce an obvious DDR in EPCs when they were expressed individually. However, we have not ruled out the possibility of the combined expression of B19V proteins, which is the case during B19V infection, and transfection of the replication-competent M20 DNAs inducing a DDR. Knockout of the 11-kDa protein in M20 DNA showed a decreased level of DNA replication in S1 cells (data not shown). We speculate that a combined expression of B19V proteins supports B19V DNA replication to the highest extent, which induces a maximum DDR. This actually is true for the NS1 protein. NS1 is essential for B19V DNA replication (Fig. 2A), but NS1 alone could not induce a DDR (Fig. 1B and C). Taken together, our results support the conclusion that the DDR induced during parvovirus infection is mediated mainly through replication of the viral genome, for which NS1 is essential.

Because EPCs are difficult to transfect (13), we delivered the B19V dsDNA genome into S1 cells by electroporation. Replication of the B19V dsDNA genome, even in the absence of ssDNA production, was sufficient to trigger a DDR in transfected S1 cells at a level similar to that observed during B19V infection. These results indicate that replication of the B19V dsDNA genome during infection of EPCs initiates the DDR independently of the production of the ssDNA viral genome. However, the ssDNA genomes of B19V and other parvoviruses have hairpin termini at both ends (20). The gap between the termini displays a structure of a single-strand break (SSB) that is recognized by ATR (15). Since it was

difficult to detect the ssDNA viral genome in the nucleus upon B19V infection (data not shown), we have not provided direct evidence that the B19V ssDNA genome elicits a DDR. However, when UV-inactivated B19V was used to infect EPCs at an MOI of 1,000 gc/cell, the same as that for the wild-type B19V in our study, neither γ-H2AX nor p-RPA32 was detected in infected cells (data not shown). It has been reported that infection of UV-inactivated AAV at a high MOI (5,000 gc/cell) elicited a DDR by mimicking the stalled replication fork (29). Further studies are warranted to determine the nature of the B19V ssDNA genome as an SSB substrate for ATR recognition.

B19V induces a DDR via replication of the RF genome, which involves replication intermediates (27) rather than via NS1 expression alone. The replication of parvovirus DNA follows the rolling-hairpin model of DNA replication, which involves a strand displacement step (19). Therefore, the formation of a replication origin complex at the replication origin, or other steps, such as nicking at the terminal resolution site by NS1 followed by unwinding of the RF DNA or hairpin by the helicase activity of NS1 (which resembles a stalled replication fork), is likely the key for triggering a DDR during virus infection. It is possible that ATR recognizes the nicked site within the terminal sequence of the genome and that the ssDNA binding protein RPA32 is recruited to the displaced ssDNA, which mimics a stalled replication fork. Thus, our observations have laid a solid foundation for further study of how replication of the ssDNA genome of autonomous parvovirus induces a DDR during virus infection.

Regulation of cell cycle progression, symbolized by arrest at the S or G_2/M phase checkpoint, is a classic strategy for infecting viruses to exploit cellular components/mechanisms to aid viral genome replication (12, 23). MVM and MVC infections activate ATM-mediated signaling, which arrests infected cells at the S and G_2/M phases; the DDR then directly leads to cell cycle arrest (1, 38). The Vpr protein of HIV is responsible for a DDR during HIV infection, which results in G_2/M arrest through ATR-checkpoint kinase 1 (Chk1) signaling (66). It is intriguing that B19V DNA replication-induced DDR does not result in G_2/M arrest, even though Chk1 and Chk2 are activated during infection (39). Therefore, our observations suggest multiple roles for virus infection-triggered DDR. In some cases, the DDR induces cell cycle arrest, which in turn facilitates virus replication or kills infected cells. In other cases, the DDR is directly involved in promoting DNA replication without arresting the cell cycle.

In summary, we have demonstrated that replication of the B19V dsDNA genome induces DDR signaling and that the DDR is dispensable for triggering cell cycle arrest during B19V DNA replication. However, the NS1 protein was instrumental in G_2/M arrest, which did not require the putative activity of endonuclease and helicase but did require TAD2 function. Furthermore, this process was independent of the p53 pathway. Further studies are needed to examine how TAD2 functions to induce G_2/M arrest and how this function coordinates with the function of the NLS to induce G_2/M arrest. Thus, B19V may have evolved a unique strategy employing NS1 to overcome difficulties in arresting the cell cycle in rapidly proliferating EPCs. The reason why the induced DDR during B19V infection of EPCs, particularly the activation of ATR and ATM signaling, did not significantly result in G_2/M arrest will be an interesting topic for future study.

ACKNOWLEDGMENTS

This work was supported in full by PHS grant R01 AI070723 from the NIAID and grant R21 HL106299 from the NHLBI to J.Q.

We are indebted to Susan Wong at the Hematology Branch, NHLBI, NIH, for helping culture $CD34^+$ human hematopoietic stem cells.

REFERENCES

1. **Adeyemi RO, Landry S, Davis ME, Weitzman MD, Pintel DJ.** 2010. Parvovirus minute virus of mice induces a DNA damage response that facilitates viral replication. PLoS Pathog. **6**:e1001141. doi:10.1371/journal.ppat.1001141.
2. **Anderson MJ, et al.** 1988. Human parvovirus B19 and hydrops fetalis. Lancet **i**:535.
3. **Banin S, et al.** 1998. Enhanced phosphorylation of p53 by ATM in response to DNA damage. Science **281**:1674–1677.
4. **Berthet C, Raj K, Saudan P, Beard P.** 2005. How adeno-associated virus Rep78 protein arrests cells completely in S phase. Proc. Natl. Acad. Sci. U. S. A. **102**:13634–13639.
5. **Block WD, Yu Y, Lees-Miller SP.** 2004. Phosphatidyl inositol 3-kinase-like serine/threonine protein kinases (PIKKs) are required for DNA damage-induced phosphorylation of the 32 kDa subunit of replication protein A at threonine 21. Nucleic Acids Res. **32**:997–1005.
6. **Bunz F, et al.** 1998. Requirement for p53 and p21 to sustain G2 arrest after DNA damage. Science **282**:1497–1501.
7. **Chaturvedi P, et al.** 1999. Mammalian Chk2 is a downstream effector of the ATM-dependent DNA damage checkpoint pathway. Oncogene **18**: 4047–4054.
8. **Chaurushiya MS, Weitzman MD.** 2009. Viral manipulation of DNA repair and cell cycle checkpoints. DNA Repair (Amst.) **8**:1166–1176.
9. **Chen AY, et al.** 2010. Role of erythropoietin receptor signaling in parvovirus B19 replication in human erythroid progenitor cells. J. Virol. **84**: 12385–12396.
10. **Chen AY, Kleiboeker S, Qiu J.** 2011. Productive parvovirus B19 infection of primary human erythroid progenitor cells at hypoxia is regulated by STAT5A and MEK signaling but not HIF alpha. PLoS Pathog. **7**:e1002088. doi:10.1371/journal.ppat.1002088.
11. **Chen AY, Luo Y, Cheng F, Sun Y, Qiu J.** 2010. Bocavirus infection induces a mitochondrion-mediated apoptosis and cell cycle arrest at G2/M phase. J. Virol. **84**:5615–5626.
12. **Chen AY, Qiu J.** 2010. Parvovirus infection-induced cell death and cell cycle arrest. Future Virol. **5**:731–741.
13. **Chen AY, et al.** 2010. The small 11kDa non-structural protein of human parvovirus B19 plays a key role in inducing apoptosis during B19 virus infection of primary erythroid progenitor cells. Blood **115**:1070–1080.
14. **Ciccia A, Elledge SJ.** 2010. The DNA damage response: making it safe to play with knives. Mol. Cell **40**:179–204.
15. **Cimprich KA, Cortez D.** 2008. ATR: an essential regulator of genome integrity. Nat. Rev. Mol. Cell Biol. **9**:616–627.
16. **Cipolleschi MG, Dello SP, Olivotto M.** 1993. The role of hypoxia in the maintenance of hematopoietic stem cells. Blood **82**:2031–2037.
17. **Collaco RF, Bevington JM, Bhrigu V, Kalman-Maltese V, Trempe JP.** 2009. Adeno-associated virus and adenovirus coinfection induces a cellular DNA damage and repair response via redundant phosphatidylinositol 3-like kinase pathways. Virology **392**:24–33.
18. **Cotmore SF, Tattersall P.** 1984. Characterization and molecular cloning of a human parvovirus genome. Science **226**:1161–1165.
19. **Cotmore SF, Tattersall P.** 2005. A rolling-haipin strategy: basic mechanisms of DNA replication in the parvoviruses, p 171–181. *In* Kerr J, Cotmore SF, Bloom ME, Linden RM, and Parrish CR (ed), Parvoviruses. Hodder Arnold, London, England.
20. **Cotmore SF, Tattersall P.** 2005. Structure and organization of the viral genome, p 73–94. *In* Kerr J, Cotmore SF, Bloom ME, Linden RM, and Parrish CR (ed), Parvoviruses. Hodder Arnold, London, England.
21. **Dahl J, You J, Benjamin TL.** 2005. Induction and utilization of an ATM signaling pathway by polyomavirus. J. Virol. **79**:13007–13017.
22. **Doerig C, Hirt B, Antonietti JP, Beard P.** 1990. Nonstructural protein of parvoviruses B19 and minute virus of mice controls transcription. J. Virol. **64**:387–396.
23. **Emmett SR, Dove B, Mahoney L, Wurm T, Hiscox JA.** 2005. The cell cycle and virus infection. Methods Mol. Biol. **296**:197–218.
24. **Fu Y, et al.** 2002. Regulation of tumor necrosis factor alpha promoter by human parvovirus B19 NS1 through activation of AP-1 and AP-2. J. Virol. **76**:5395–5403.

25. **Gareus R, et al.** 1998. Characterization of cis-acting and NS1 protein-responsive elements in the p6 promoter of parvovirus B19. J. Virol. **72**:609–616.
26. **Guan W, et al.** 2008. Block to the production of full-length B19 virus transcripts by internal polyadenylation is overcome by replication of the viral genome. J. Virol. **82**:9951–9963.
27. **Guan W, Wong S, Zhi N, Qiu J.** 2009. The genome of human parvovirus B19 virus can replicate in non-permissive cells with the help of adenovirus genes and produces infectious virus. J. Virol. **83**:9541–9553.
28. **Guo YM, et al.** 2010. CpG-ODN 2006 and human parvovirus B19 genome consensus sequences selectively inhibit growth and development of erythroid progenitor cells. Blood **115**:4569–4579.
29. **Jurvansuu J, Raj K, Stasiak A, Beard P.** 2005. Viral transport of DNA damage that mimics a stalled replication fork. J. Virol. **79**:569–580.
30. **Kaufmann B, Chipman PR, Kostyuchenko VA, Modrow S, Rossmann MG.** 2008. Visualization of the externalized VP2 N termini of infectious human parvovirus B19. J. Virol. **82**:7306–7312.
31. **Kaufmann B, Simpson AA, Rossmann MG.** 2004. The structure of human parvovirus B19. Proc. Natl. Acad. Sci. U. S. A. **101**:11628–11633.
32. **Larkin MA, et al.** 2007. Clustal W and Clustal X version 2.0. Bioinformatics **23**:2947–2948.
33. **Legendre D, Rommelaere J.** 1994. Targeting of promoters for trans activation by a carboxy-terminal domain of the NS-1 protein of the parvovirus minute virus of mice. J. Virol. **68**:7974–7985.
34. **Lilley CE, Schwartz RA, Weitzman MD.** 2007. Using or abusing: viruses and the cellular DNA damage response. Trends Microbiol. **15**:119–126.
35. **Liu Q, et al.** 2000. Chk1 is an essential kinase that is regulated by Atr and required for the G(2)/M DNA damage checkpoint. Genes Dev. **14**:1448–1459.
36. **Lou S, et al.** 2012. Molecular characterization of the newly identified human parvovirus 4 in the family Parvoviridae. Virology **422**:59–69.
37. **Luo W, Astell CR.** 1993. A novel protein encoded by small RNAs of parvovirus B19. Virology **195**:448–455.
38. **Luo Y, Chen AY, Qiu J.** 2011. Bocavirus infection induces a DNA damage response that facilitates viral DNA replication and mediates cell death. J. Virol. **85**:133–145.
39. **Luo Y, et al.** 2011. Parvovirus B19 infection of human primary erythroid progenitor cells triggers ATR-Chk1 signaling, which promotes B19 virus replication. J. Virol. **85**:8046–8055.
40. **Mah LJ, El-Osta A, Karagiannis TC.** 2010. gammaH2AX: a sensitive molecular marker of DNA damage and repair. Leukemia **24**:679–686.
41. **Moffatt S, et al.** 1996. A cytotoxic nonstructural protein, NS1, of human parvovirus B19 induces activation of interleukin-6 gene expression. J. Virol. **70**:8485–8491.
42. **Moffatt S, Yaegashi N, Tada K, Tanaka N, Sugamura K.** 1998. Human parvovirus B19 nonstructural (NS1) protein induces apoptosis in erythroid lineage cells. J. Virol. **72**:3018–3028.
43. **Momoeda M, Wong S, Kawase M, Young NS, Kajigaya S.** 1994. A putative nucleoside triphosphate-binding domain in the nonstructural protein of B19 parvovirus is required for cytotoxicity. J. Virol. **68**:8443–8446.
44. **Morey AL, Fleming KA.** 1992. Immunophenotyping of fetal haemopoietic cells permissive for human parvovirus B19 replication in vitro. Br. J. Haematol. **82**:302–309.
45. **Morita E, Nakashima A, Asao H, Sato H, Sugamura K.** 2003. Human parvovirus B19 nonstructural protein (NS1) induces cell cycle arrest at G(1) phase. J. Virol. **77**:2915–2921.
46. **Morita E, Sugamura K.** 2002. Human parvovirus B19-induced cell cycle arrest and apoptosis. Springer Semin. Immunopathol. **24**:187–199.
47. **Morita E, et al.** 2001. Human parvovirus B19 induces cell cycle arrest at G(2) phase with accumulation of mitotic cyclins. J. Virol. **75**:7555–7563.
48. **Nakashima A, Morita E, Saito S, Sugamura K.** 2004. Human parvovirus B19 nonstructural protein transactivates the p21/WAF1 through Sp1. Virology **329**:493–504.
49. **Orba Y, et al.** 2010. Large T antigen promotes JC virus replication in G2-arrested cells by inducing ATM- and ATR-mediated G2 checkpoint signaling. J. Biol. Chem. **285**:1544–1554.
50. **Ozawa K, et al.** 1987. Novel transcription map for the B19 (human) pathogenic parvovirus. J. Virol. **61**:2395–2406.
51. **Ozawa K, Kurtzman G, Young N.** 1986. Replication of the B19 parvovirus in human bone marrow cell cultures. Science **233**:883–886.
52. **Parmar K, Mauch P, Vergilio JA, Sackstein R, Down JD.** 2007. Distribution of hematopoietic stem cells in the bone marrow according to regional hypoxia. Proc. Natl. Acad. Sci. U. S. A. **104**:5431–5436.
53. **Pillet S, et al.** 2004. Hypoxia enhances human B19 erythrovirus gene expression in primary erythroid cells. Virology **327**:1–7.
54. **Piskacek S, et al.** 2007. Nine-amino-acid transactivation domain: establishment and prediction utilities. Genomics **89**:756–768.
55. **Raab U, et al.** 2002. NS1 protein of parvovirus B19 interacts directly with DNA sequences of the p6 promoter and with the cellular transcription factors Sp1/Sp3. Virology **293**:86–93.
56. **Ruiz Z, Mihaylov IS, Cotmore SF, Tattersall P.** 2011. Recruitment of DNA replication and damage response proteins to viral replication centers during infection with NS2 mutants of Minute Virus of Mice (MVM). Virology **410**:375–384.
57. **Sancar A, Lindsey-Boltz LA, Unsal-Kacmaz K, Linn S.** 2004. Molecular mechanisms of mammalian DNA repair and the DNA damage checkpoints. Annu. Rev. Biochem. **73**:39–85.
58. **Schneider H.** 2011. Oxygenation of the placental-fetal unit in humans. Respir. Physiol. Neurobiol. **178**:51–58.
59. **Schwartz RA, Carson CT, Schuberth C, Weitzman MD.** 2009. Adeno-associated virus replication induces a DNA damage response coordinated by DNA-dependent protein kinase. J. Virol. **83**:6269–6278.
60. **Shieh SY, Ikeda M, Taya Y, Prives C.** 1997. DNA damage-induced phosphorylation of p53 alleviates inhibition by MDM2. Cell **91**:325–334.
61. **Smith J, Tho LM, Xu N, Gillespie DA.** 2010. The ATM-Chk2 and ATR-Chk1 pathways in DNA damage signaling and cancer. Adv. Cancer Res. **108**:73–112.
62. **Sol N, et al.** 1999. Possible interactions between the NS-1 protein and tumor necrosis factor alpha pathways in erythroid cell apoptosis induced by human parvovirus B19. J. Virol. **73**:8762–8770.
63. **Srivastava A, Lu L.** 1988. Replication of B19 parvovirus in highly enriched hematopoietic progenitor cells from normal human bone marrow. J. Virol. **62**:3059–3063.
64. **St Amand AJ, Astell CR.** 1993. Identification and characterization of a family of 11-kDa proteins encoded by the human parvovirus B19. Virology **192**:121–131.
65. **Stucki M, Jackson SP.** 2006. gammaH2AX and MDC1: anchoring the DNA-damage-response machinery to broken chromosomes. DNA Repair (Amst.) **5**:534–543.
66. **Tachiwana H, et al.** 2006. HIV-1 Vpr induces DNA double-strand breaks. Cancer Res. **66**:627–631.
67. **Takubo K, et al.** 2010. Regulation of the HIF-1alpha level is essential for hematopoietic stem cells. Cell Stem Cell **7**:391–402.
68. **Tijssen P, et al.** 2012. Family Parvoviridae, p 405–425. *In* King AM, Lefkowitz E, Adams MJ, Carstens EB (ed), Virus taxonomy: ninth report of the International Committee on Taxonomy of Viruses. Elsevier, London, United Kingdom.
69. **Walker SL, Wonderling RS, Owens RA.** 1997. Mutational analysis of the adeno-associated virus type 2 Rep68 protein helicase motifs. J. Virol. **71**:6996–7004.
70. **Wan Z, et al.** 2010. Human parvovirus B19 causes cell cycle arrest of human erythroid progenitors via deregulation of the E2F family of transcription factors. J. Clin. Invest. **120**:3530–3544.
71. **Weitzman MD, Lilley CE, Chaurushiya MS.** 2010. Genomes in conflict: maintaining genome integrity during virus infection. Annu. Rev. Microbiol. **64**:61–81.
72. **Wong S, et al.** 2008. Ex vivo-generated CD36+ erythroid progenitors are highly permissive to human parvovirus B19 replication. J. Virol. **82**:2470–2476.
73. **Yaegashi N, et al.** 1999. Parvovirus B19 infection induces apoptosis of erythroid cells in vitro and in vivo. J. Infect. **39**:68–76.
74. **Young NS, Brown KE.** 2004. Parvovirus B19. N. Engl. J. Med. **350**:586–597.
75. **Zadori Z, et al.** 2001. A viral phospholipase A2 is required for parvovirus infectivity. Dev. Cell **1**:291–302.
76. **Zhao RY, Elder RT.** 2005. Viral infections and cell cycle G2/M regulation. Cell Res. **15**:143–149.
77. **Zhao X, et al.** 2008. Ataxia telangiectasia-mutated damage-signaling kinase- and proteasome-dependent destruction of Mre11-Rad50-Nbs1 subunits in simian virus 40-infected primate cells. J. Virol. **82**:5316–5328.
78. **Zhi N, et al.** 2006. Molecular and functional analyses of a human parvovirus B19 infectious clone demonstrates essential roles for NS1, VP1, and the 11-kilodalton protein in virus replication and infectivity. J. Virol. **80**:5941–5950.
79. **Zhi N, et al.** 2010. Codon optimization of human parvovirus B19 capsid genes greatly increases their expression in nonpermissive cells. J. Virol. **84**:13059–13062.
80. **Zhi N, Zadori Z, Brown KE, Tijssen P.** 2004. Construction and sequencing of an infectious clone of the human parvovirus B19. Virology **318**:142–152.